

A BRIEF OVERVIEW OF SCANNING TRANSMISSION ELECTRON MICROSCOPY IN A SCANNING ELECTRON MICROSCOPE

Jason Holm

National Institute of Standards and Technology

jason.holm@nist.gov

INTRODUCTION

Scanning electron microscopes (SEMs) and the transmission electron detectors used therein are widely available. Both are generally easy to use, making the collection of imaging and diffraction techniques referred to as scanning transmission electron microscopy in a scanning electron microscope (STEM-in-SEM) more accessible today than ever before. These techniques are well suited to a host of applications including, for example, nanoparticle metrology,^[1] imaging beam sensitive materials,^[2] grain texture studies,^[3] and defect analyses.^[4]

In this article, some of the pros and cons of STEM-in-SEM and recent advancements in detector technology are described. To illustrate imaging and diffraction capabilities of STEM-in-SEM, a few applications are shown including 4dimensional (4D) STEM-in-SEM, a recently developed method that leverages both real and diffraction space to obtain useful information.

STEM-IN-SEM

Scanning electron microscopes (SEMs) are ubiquitous in laboratories. The wide array of signals and the numerous detectors available to collect those signals for imaging and analytical studies make SEMs practically indispensable. Many SEMs are also equipped with a focused ion beam (FIB) column that enables electron transparent samples to be extracted from specific locations in bulk samples. Additionally, the number of SEMs equipped with detectors enabling transmission electron imaging and diffraction is increasing rapidly, and for good reason. Combined, the SEM and its various detectors, a FIB, and a transmission detector provide a powerful combination of instruments for sample preparation, imaging, diffraction, and analysis with practical length scales spanning

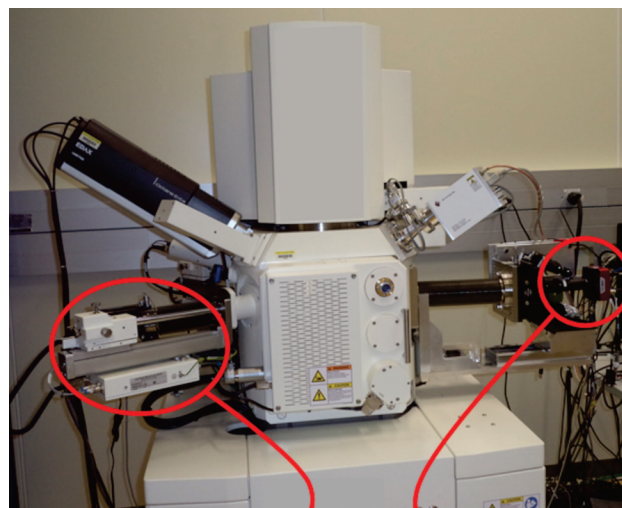
nanometers to several centimeters. Moreover, these capabilities can be implemented without removing the sample from the SEM vacuum chamber.

Although scanning transmission imaging was an early sample visualization mode in SEMs,^[5] it was rapidly overshadowed by advancements in transmission electron microscopy (TEM) and eventually higher energy (i.e., > 100 keV) scanning transmission electron microscopy (STEM). Within the last couple decades, however, STEM-in-SEM (referred to as such to differentiate it from higher energy STEM platforms) has seen an increasingly rapid revival starting approximately with the works by Morandi and Merli, who studied contrast in semiconductor multilayer structures.^[6] Shortly thereafter, transmission Kikuchi diffraction (TKD) methods in an SEM were described.^[7,8] This technique is commonly used for phase and grain orientation mapping in crystalline samples. The order of magnitude improvement in spatial resolution reported in transmission mode compared to conventional backscatter detection mode (i.e., ~ 2 nm compared to a couple tens of nanometers) made this technique especially appealing for electron transparent samples. Advancements in solid-state detector technology for transmission imaging were happening simultaneously, and today every SEM vendor offers on-axis solid-state detectors for transmission imaging. Some SEMs also have multiple transmission detectors (Fig. 1).

STEM-in-SEM is a logical combination of conventional SEM and higher energy STEM technology, and it makes sense to leverage developments made in other platforms to the SEM. For example, electron scattering physics is effectively the same at SEM energies as it is at STEM energies provided the sample is sufficiently thin. Therefore, the extensive theory developed to understand transmission

electron imaging and diffraction and the technologies developed for electron beam control can conceivably be utilized in a STEM-in-SEM setting. Although the current level of lens control (i.e., beam spot size, no post-sample lenses, and lack of aberration correction) does not enable atomic resolution imaging or some of the specialized imaging modes, STEM-in-SEM imaging capabilities are extensive and not limited to bright-field (BF) and dark-field (DF) imaging. In cases where users require more beam positioning control or automation than included in the SEM software user interface, most SEM vendors offer an application programming interface (API) which can extend the beam positioning capabilities, and external scan generators can also be implemented for even more control. For example, arbitrary scan patterns can be implemented to accommodate low-dose imaging techniques. Although the current state of the art in SEM beam control is good (Figs. 2a-c show how the beam can be adjusted to obtain different diffraction conditions), it is only a matter of time before free-lens control and aberration correction are offered on new SEMs.

A major benefit of STEM-in-SEM is vacuum chamber size. Ample room is often available for in situ or operando experiments, custom sample holders, and detectors.^[9-13] Several access ports to the vacuum chamber are generally also available, and other sample manipulation and measurement tools can be added or removed depending



Solid-state detector
for imaging

CMOS camera
for diffraction

Fig. 1 An SEM equipped with two transmission detectors for imaging and diffraction.

on experimental requirements. Moreover, sample sizes are not limited to 3 mm diameter configurations. Electron transparent samples of nearly any shape or size can be used provided that the sample can be supported between the pole piece and transmission detector, and multiple samples can be loaded and analyzed for high throughput analysis with the appropriate holder.

(continued on page 22)

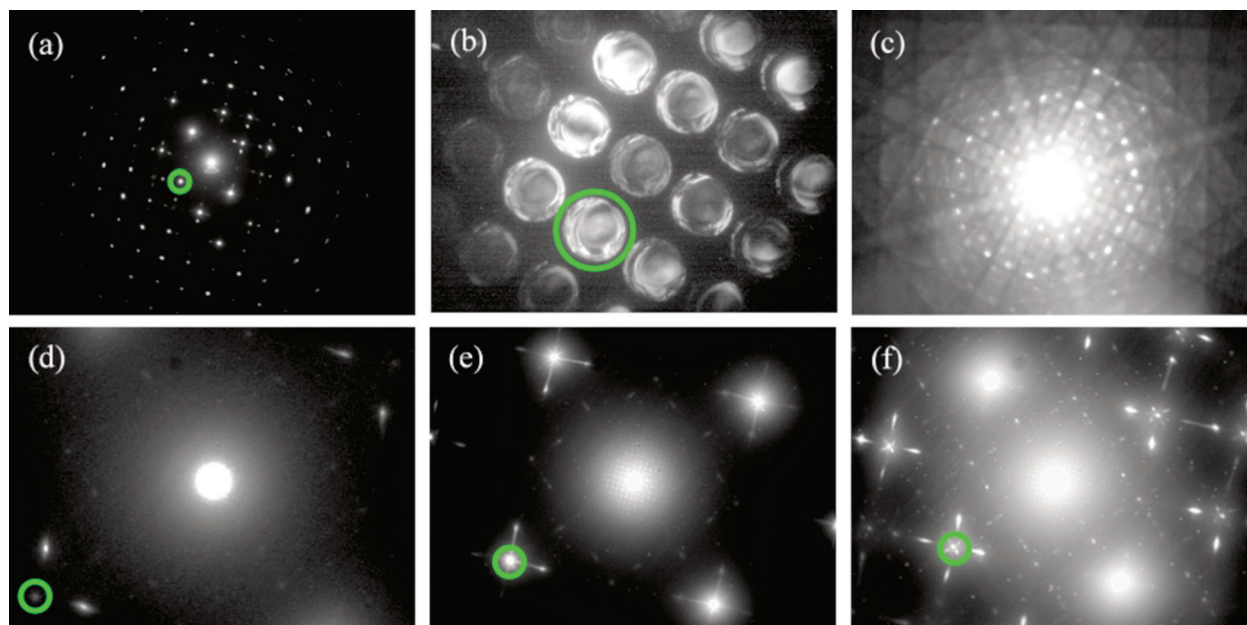


Fig. 2 Au (001) foil DPs. Inset green circles indicate the [020] reflection. The direct beam is located approximately at the center of each image. (a) A 30 keV DP obtained with $CL \approx 7.5$ mm and underfocused beam (i.e., working distance = 50 mm for quasi-parallel illumination). (b) A 30 keV convergent beam DP with beam convergence angle $\alpha \approx 10$ mrad. (c) A 30 keV DP with illumination set to emphasize Kikuchi scattering. Spot patterns obtained using a 7.5 mm aperture, $CL \approx 25$ mm, and beam energies of (d) 10 keV, (e) 20 keV, (f) 30 keV. Note the satellite spots and other fine details between kinematically allowed reflections.

SCANNING TRANSMISSION ELECTRON MICROSCOPY *(continued from page 19)*

STEM-in-SEM is also considered a low-voltage electron imaging and diffraction technique. Beam energy limits for transmission detectors range from a practical minimum of approximately 5 keV to at least 30 keV (i.e., the maximum beam energy in modern SEMs). Some detectors can operate at lower energy detection thresholds, but the practical low end depends on factors including detector sensitivity, exposure time, beam current, and sample mass-thickness. As with all transmission imaging, samples should be as thin as possible, and this is especially important at low voltages. Benefits of lowering the beam energy include increased electron scattering probability, larger characteristic scattering angles, and little to no knock-on damage. For example, electron scattering by a sample is more likely at 30 keV than 100 keV, and the increased scattering probability can produce stronger image contrast, which can be useful for samples comprising low atomic number materials. Figures 2d-f show how characteristic scattering angles change with beam energy for an Au (001) foil. Notice how the spacing between diffraction spots increases as the beam energy decreases, and that numerous spots and streaks are visible around the primary reflections that aren't commonly observed at higher energies.

Because there are no lenses between the sample and the transmission detector in an SEM, the camera length (CL) is used for diffraction pattern (DP) magnification

(i.e., compare Fig. 2a and Fig. 2f). CL is defined here as the distance between the sample and the effective image plane.^[14] A typical CL range is approximately 2 to 25 mm depending on the size of the vacuum chamber and the sample stage.

Ultimately, greater scattering probability means that more information can be gleaned from a sample provided that the sample is not damaged by the electron scattering process. To that end, although the knock-on damage threshold for many materials is greater than the maximum SEM beam energy,^[15] ionization damage may still be a concern in some instances. For example, zeolites are susceptible to ionization damage at low beam energies.^[16] The damage is observed most readily as a reduction in DP spot intensity with increasing beam exposure. However, low-dose methods can be used to minimize beam damage and still allow the collection of meaningful information.^[17]

DETECTORS

Solid-state diode detectors are by far the most common transmission detector for STEM-in-SEM imaging. These devices generally enable BF, DF, and annular dark-field (ADF) imaging with concentric annular diodes. The annular diodes are commonly segmented into quadrants, and signals from the different segments can be combined to highlight material composition differences. High-angle annular dark field (HAADF) imaging for atomic number

contrast (i.e., Z-contrast) is generally feasible with these detectors. Provided that coherent scattering is largely absent from the HAADF signal, the image intensity, I , is approximately proportional to $Z^{1.8}$.^[18] One major benefit of the solid-state detectors is the high signal-to-noise ratio that lends itself to sharp, strong contrast images. Another benefit is the high bandwidth that can enable video recording in some instances. Although they are intended for imaging, a simple masking system can be used to glean diffraction information for applications such as texture or grain orientation mapping.^[19,20]

Except for TKD applications, detectors intended specifically for diffraction are not yet offered

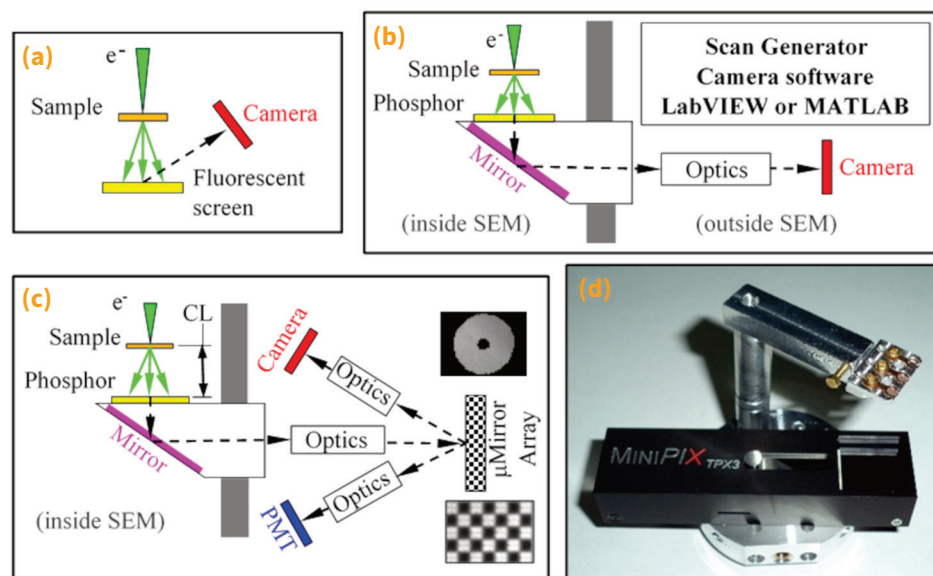


Fig. 3 Schematics and images of various detectors for STEM-in-SEM. (a) An approach similar to viewing DPs by eye in a TEM where a camera is used instead of binoculars. (b) A modified TKD system for diffraction. (c) A modified TKD system for imaging and diffraction. The inset images show mirrors tilted to the PMT comprising a 2 x 2 matrix (bottom) and an annular aperture (top). (d) A small footprint direct electron detector mounted on a multi-stub sample holder. Standoffs can be added or removed to adjust the camera length (CL) of the 3-position sample holder.

by most major SEM vendors. However, implementing an on-axis transmission detector can be as straightforward as using a fluorescent screen and a digital camera (Fig. 3a).^[9] Still, diffraction in an SEM presents a few challenges. For example, although it isn't as easy as in a TEM or a STEM, changing between quasi-parallel illumination used to obtain sharp diffraction spots or rings and convergent illumination to obtain convergent beam electron diffraction (CBED) patterns or to emphasize Kikuchi scattering is possible in an SEM by changing the beam limiting aperture size and the working distance (Fig. 2). To that end, beam convergence angles from less than 1 milliradian (i.e., ~ 0.06 degrees) to more than 60 milliradians can be obtained in most SEMs.

A recent detector development involved the adaptation of a conventional EBSD detector for transmission imaging.^[11] Here, a phosphor centered on the optic axis is positioned below the sample (Fig. 3b). When electrons transmitted through the sample strike the phosphor, the electron scattering distribution (i.e., the DP) is replicated in the photon distribution emitted by the phosphor. A mirror and lens assembly is used to image the photon distribution to a digital camera positioned outside the vacuum chamber. Although this detector has primarily been used for TKD applications, it can be used in a variety of ways for recording and combining DPs, including 4D STEM-in-SEM. For example, the DPs in Figs. 2 and 5 were recorded using this setup.

A significant advancement of the phosphor-based detector was recently described.^[12] Here, a digital micromirror device (DMD), a digital camera, and a photomultiplier tube (PMT) enable imaging and diffraction in one programmable STEM (p-STEM) detector (Fig. 3c). The DMD comprises an array of micromirrors, each of which can be independently tilted towards the camera or the PMT. When all mirrors are aimed towards the camera, the system is in diffraction mode and can be used for TKD or other diffraction-based analyses including 4D STEM-in-SEM. When user-specified mirrors are tilted towards the PMT, the system is in imaging mode where the photon signal reflected to the PMT is proportional to image intensity at each beam raster point. One benefit of this system is that images from any detector on the SEM can be used to choose where to collect DPs from on the sample. The user simply clicks on specific points or selects a region of interest (ROI) on the image, and DPs are automatically recorded at each position or ROI (Fig. 4). Those DPs can then be used on the fly to select specific spots for DF imaging, where the appropriate mirrors are tilted to the PMT for real-space imaging. Virtual aperture implementation can also be automated by use of a suitable software script.

The most recent development in detector technology for STEM-in-SEM is perhaps the incorporation of direct electron detection methods.^[10] These small, pixelated, radiation cameras can be placed under the sample on the optic axis to record the position, energy, and time of

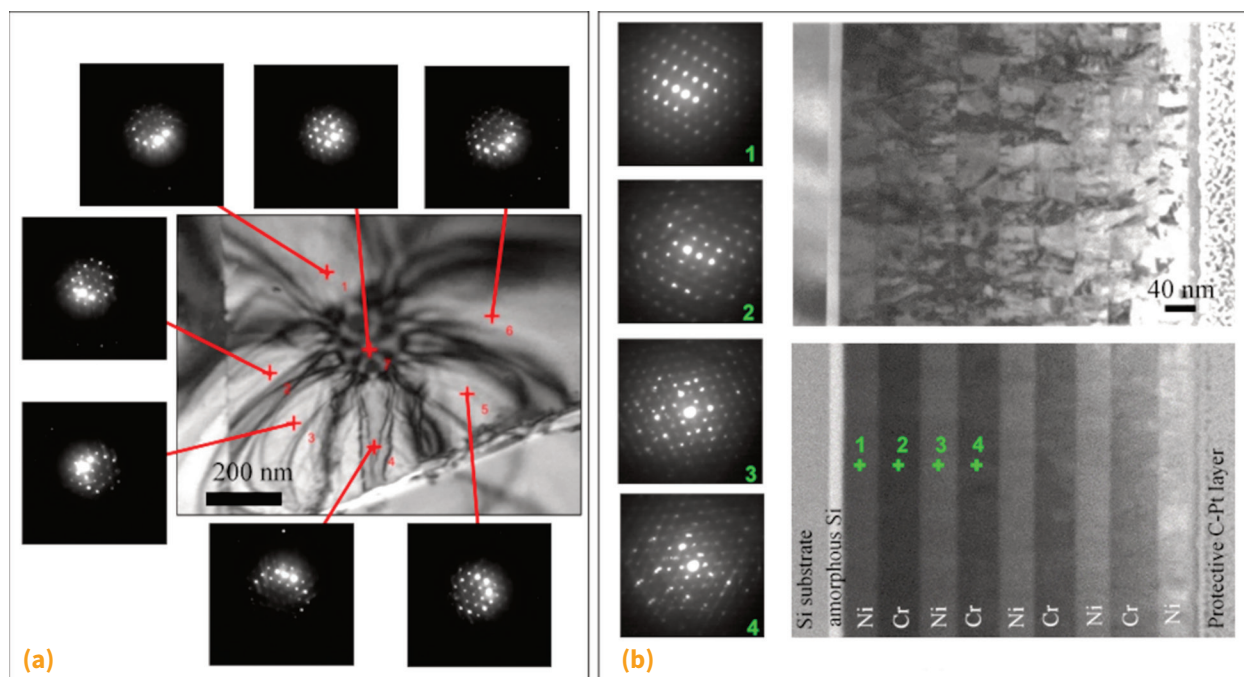


Fig. 4 Transmission images and DPs obtained with the p-STEM detector. (a) A bend center in stainless steel. (b) A Ni-Cr thin film depth profile standard. The top image shows a 010 milliradian BF image, the bottom a 50 to 100 milliradian ADF image. Inset numbers and crosses indicate positions where the diffractions patterns were obtained.

each detected electron. In addition to the vendor-supplied user interface, a python interface is available for custom operations. The practically unlimited dynamic range of this detector is an advantage over the other detectors described here, as is the potential for hyperspectral energy-based measurements/images (which have not

yet been explored in an SEM). Although the frame rate and pixel size are not yet at the same level as high-end CMOS camera technology or other high-speed diffraction cameras currently used in TEMs or STEMs, the convenience of an extremely small footprint and ease of use are advantageous (Fig. 3d). A more advanced implementation

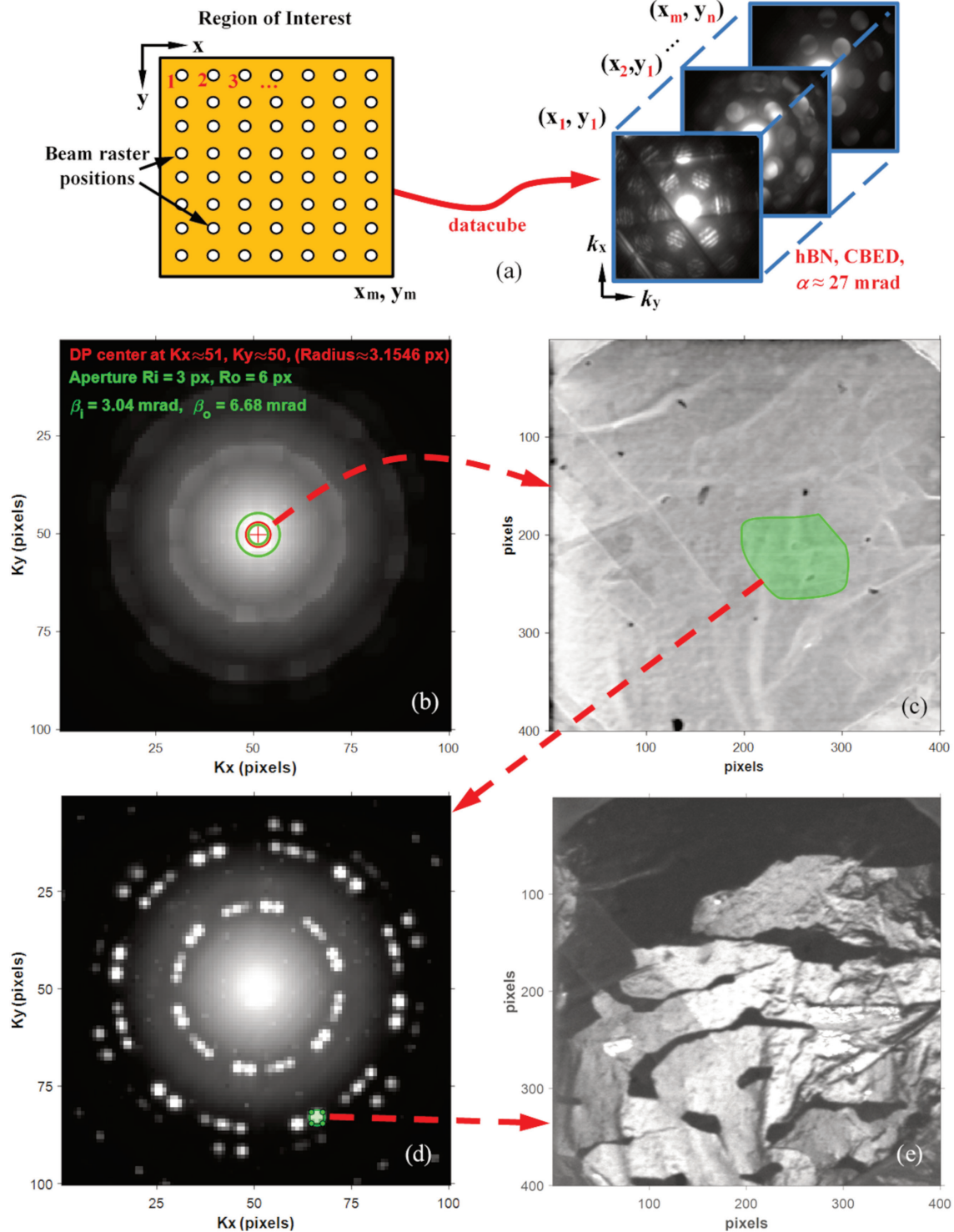


Fig. 5 4D STEM-in-SEM. (a) Experimental schematic. (b) The average DP from the dataset of a two-dimensional MoS_2 sample. The inset red circle and cross shows the direct beam center and approximate spot size. The inset green circles indicate the virtual annular aperture used to create (c) a marginal BF image. (d) The average DP of the ROI indicated in (b). (e) A DF image showing regions of the sample that scatter electrons into the small spot indicated in (d).

enabling motorized sample manipulation (i.e., tilt, rotate, CL) could be realized by combining this detector with a six degree-of-freedom apparatus described recently.^[13]

4D STEM-IN-SEM IMAGING AND DIFFRACTION

As mentioned, numerous transmission imaging techniques can be implemented in an SEM. Seeing as many readers are familiar with common solid-state detectors and the concomitant imaging modes, those applications will not be covered. An emerging method that has gained popularity is 4D STEM (or 4D STEM-in-SEM as it pertains here), a recently coined name for a technique encompassing several applications.^[21] Here, a DP is recorded at each raster position as the electron beam is scanned across a sample, and those patterns are stored in a data cube for offline analyses (Fig. 5a).

As an introduction to 4D STEM-in-SEM, one way of visualizing the data in real and reciprocal space (i.e., k-space) is shown in Fig. 5. Here, a MATLAB script was used to determine and display the average DP of the entire dataset from a multilayer two-dimensional MoS₂ sample (Fig. 5b) and an annular image was compiled from the dataset (Fig. 5c). The average DP generally provides a broad overview of the sample structure, but it may also be overwhelming, so the script allows the user to select an ROI from the real space image to limit the dataset for subsequent analyses. For example, a less complex DP from the region specified in Fig. 5c is shown in Fig. 5d. A virtual aperture can then be drawn on the reduced dataset, and a real-space image showing regions of the sample that scatter electrons into the user-selected region can be extracted from the reduced dataset (Fig. 5e). Like the p-STEM detector, the 4D STEM-in-SEM virtual aperture can be any shape. Perhaps more importantly though, the data can be analyzed in any number of ways without concern for incurring further damage to beam sensitive samples.

Although difficult to show in print, a convenient way to survey the data/sample is to create animated image sequences that the user can specify. For example, the script used here enables the user to draw a freehand line on any DP and to specify a virtual aperture. The script scans the virtual aperture along each beam raster point in the line, extracts a real-space image at each point, and writes the image to an image stack that can be replayed in an animated format. Alternatively, a freehand line can be drawn on a real-space image and the DPs along that line can be visualized in the same manner.

4D STEM-in-SEM is not without challenges, however, two of which are stage drift and data storage. Because

diffraction cameras available for SEMs are currently limited to approximately 1000 frames per second, scan times can last from a few minutes to more than an hour depending on the camera binning and the number of points in the raster array. Almost any SEM sample stage can drift several tens of nanometers in an hour. Data files can also be large, making storage and data analysis potentially cumbersome. For example, a single dataset file size can easily comprise several tens of gigabytes depending on the scan resolution, camera binning, camera ROI, etc. Processing times can be improved by setting aside unneeded data, by using every other DP, or by binning DPs together. However, the vast amount of diffraction data is a major benefit of the technique, and numerous applications have been devised to take full advantage of the information including monolayer graphene grain orientation mapping,^[22] strain mapping,^[23] and non-contact nanoscale temperature mapping,^[24] for example. Furthermore, numerous python scripts are available online to analyze 4D datasets (i.e., LiberTEM, pyxem, py4Dstem, hyperspy, pycroscopy, etc.).

SUMMARY

STEM-in-SEM imaging and diffraction techniques are accessible today, and their utility continues to expand. Although there will always be the need for high-energy STEM/TEM, the SEM can fulfill many transmission electron imaging and diffraction needs provided that the sample is sufficiently thin. In addition to the solid-state detectors for imaging, new diffraction detectors continue to appear that will inevitably be a standard option on all SEMs. Regarding 4D STEM-in-SEM, the vast amount of data collected in each dataset offers many opportunities for further exploration beyond the existing applications, and it is only a matter of time before faster diffraction cameras are implemented in an SEM.

ACKNOWLEDGMENT

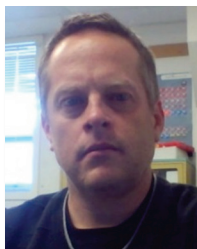
Identification of commercial products does not imply recommendation or endorsement by the National Institute of Standards and Technology, nor does it imply the products are the best suited for the application.

REFERENCES

1. E. Buhr, et al.: "Characterization of Nanoparticles by Scanning Electron Microscopy in Transmission Mode," *Meas. Sci. Technol.*, 2009, 20, p. 084025.
2. M. Kuwajima, et al.: "Automated Transmission-Mode Scanning Electron Microscopy (tSEM) for Large Volume Analysis at Nanoscale Resolution," *PLOS ONE*, 2013, 8, p. e5957.
3. R.H. Geiss, et al.: "Transmission EBSD in the Scanning Electron Microscope," *Microscopy Today*, 2013, 21, p. 16-20.
4. C. Sun, et al.: "Analysis of Crystal Defects by Scanning Transmission Electron Microscopy (STEM) in a Modern Scanning Electron Microscope," *Adv. Struct. Chem. Imag.*, 2019, 5(1).

5. D. McMullan: Scanning Electron Microscopy 1928-1965, *Scanning*, 1995, 17, p. 175-185.
6. P. G. Merli, et al.: *Ultramicroscopy*, 2003, 94, p. 89-98.
7. R.R. Keller, et al.: "Transmission Electron Diffraction From Nanoparticles, Nanowires and Thin Films in an SEM With Conventional EBSD Equipment," *Microsc. Microanal.*, 2010, 116(S2), p. 742-1743.
8. P. Trimby: "Orientation Mapping of Nanostructured Materials using Transmission Kikuchi Diffraction in the Scanning Electron Microscope," *Ultramicroscopy*, 2012, 1210, p. 16-24.
9. P. Schweitzer, et al.: "Low Energy Nano Diffraction (LEND) - A Versatile Diffraction Technique in SEM," *Ultramicroscopy*, 2020, 213, p. 112956.
10. A. Orekhov, et al.: "Wide Field of View Crystal Orientation Mapping of Layered Materials," <https://arxiv.org/abs/2011.01875>.
11. E. Brodu, et al.: "On-axis TKD for Orientation Mapping of Nanocrystalline Materials in SEM," *Matls. Char.*, 2017, 130, p. 92-96.
12. B. Caplins, et al.: "Transmission Imaging with a Programmable Detector in a Scanning Electron Microscope," *Ultramicroscopy*, 2019, 196, p. 40-48.
13. J. Müller, et al.: "Features of Our SEM Transmission Diffraction Substage with 6-axis Sample Control and a Camera with Variable Camera Length," *Microsc. Microanal.*, 2020, 26(S2), p. 1906-1907.
14. J. Holm and B. Caplins: "STEM in SEM: Introduction to Scanning Transmission Electron Microscopy for Microelectronics Failure Analysis," 2020, <https://doi.org/10.31399/asm.tb.stemsem.9781627082921>
15. R.F. Egerton, et al.: "Radiation Damage in the TEM and SEM," *Micron*, 2004, 35, p. 399-409.
16. O. Ugurlu, et al.: "Radiolysis to Knock-on Damage Transition in Zeolites under Electron Beam Irradiation," *Phys. Rev. B*, 2011, 83, p. 113408.
17. J. Holm: "STEM-in-SEM Imaging and Diffraction with Extremely Beam Sensitive Ultrathin Zeolites," *Microsc. Microanal.*, submitted for publication 2021.
18. J. Liu and J.M. Cowley: "Imaging with High-angle Scattered Electrons and Secondary Electrons in the STEM," *Ultramicroscopy*, 1991, 37, p. 50-71.
19. J. Holm, and R.R. Keller: "Angularly-selective Transmission Imaging in a Scanning Electron Microscope," *Ultramicroscopy*, 2016, 167, p. 43-56.
20. B. Caplins, et al.: "Orientation Mapping of Graphene in a Scanning Electron Microscope," *Carbon*, 2019, 149, p. 400-406.
21. H. Yang, et al.: "4D STEM: High Efficiency Phase Contrast Imaging using a Fast Pixelated Detector," *Journal of Physics: Conference Series*, 2015, 644, p. 012032.
22. B. Caplins, J. Holm, R. White, and R. Keller: "Orientation Mapping of Graphene using 4D STEM-in-SEM," *Ultramicroscopy*, 2020, 219, p. 113137.
23. Ozdol, et al.: "Four-Dimensional Scanning Transmission Electron Microscopy (4D-STEM): From Scanning Nanodiffraction to Ptychography and Beyond," *Microsc. Microanal.*, 2019, 25, p. 563-582.
24. G. Wehmeyer, et al., "Measuring Temperature-dependent Thermal Diffuse Scattering using Scanning Transmission Electron Microscopy," *Appl. Phys. Lett.*, 2018, 113, p. 253101.

ABOUT THE AUTHOR



Jason D. Holm returned to academia to earn a Ph.D. from the University of Minnesota in mechanical engineering with a nanotechnology emphasis, after working several years in industry as a mechanical engineer. He is currently a staff member at the National Institute of Standards and Technology (NIST) in the Nanoscale Reliability Group where he works as a materials research engineer.